




Effects of Different Formulation Methods on Drug Crystallinity, Drug-Carrier Interaction, and Ex Vivo Permeation of a Ternary Solid Dispersion Containing Nisoldipine

May Kyaw Oo¹ · Syed Mahmood^{2,3} · Wong Tin Wui⁴ · Uttam Kumar Mandal⁵ · Bappaditya Chatterjee^{1,6} 

Published online: 12 December 2019

© Springer Science+Business Media, LLC, part of Springer Nature 2019

Abstract

Background Solid dispersion (SD) is an established approach to increase the solubility and dissolution of BCS class II drugs. The selection of a suitable method of preparation and the suitable polymeric carrier are the two most important parameters for a successful SD. The present research is aimed to evaluate the effect of preparation method on drug crystallinity, drug-polymer interaction, ex vivo permeability, and SD stability.

Method A ternary SD containing nisoldipine as drug and PVP K30, poloxamer 188 as the carrier was prepared by hot melt mixing, solvent evaporation by rotary vacuum evaporator, and lyophilization. The prepared samples were analyzed in comparison in order to meet the objectives.

Results All three methods yielded a mixed system of the crystalline and amorphous phase with a significant increase in saturation solubility compared to the raw drug. Infra-red spectroscopy study showed the highest degree of H bonding between drug and carrier in the freeze-dried formulation. X-ray diffraction study showed maximum loss of drug crystallinity from the rotary vacuum evaporated SD (3.70% at 11.3, 2θ angle). Ex vivo permeability study showed the maximum drug permeation by freeze-dried product. But freeze-dried product was shown to be the least stable in stability analysis. In terms of product stability, melt mixing is the best out of the three methods tested.

Conclusion Different methods of preparation have different impacts on functional group interaction, loss of crystallinity, ex vivo permeation, and stability of ternary SD.

Keywords Nisoldipine · Solid dispersion · Ex vivo permeability study · Drug-carrier interaction

✉ Bappaditya Chatterjee
bdpharmaju@gmail.com

- ¹ Kulliyyah of Pharmacy, International Islamic University Malaysia, 25200 Kuantan, Malaysia
- ² Department of Pharmaceutical Engineering, Faculty of Chemical and Process Engineering Technology, University Malaysia Pahang, 26300 Gambang, Malaysia
- ³ Centre of Excellence for Advanced Research in Fluid Flow (CARIFF), University Malaysia Pahang, 26300 Gambang, Malaysia
- ⁴ Non-destructive Biomedical and Pharmaceutical Research Centre, iPROMISE, Universiti Teknologi MARA, 42300 Puncak Alam, Selangor, Malaysia
- ⁵ Department of Pharmaceutical Sciences & Technology, Maharaja Ranjit Singh Punjab Technical University (MRSPTU), Bathinda 151001, India
- ⁶ Pharmaceutics Department, Shobhaben Pratapbhai Patel School of Pharmacy & Technology Management (SPSPTM), SVKM'S NMIMS, Mumbai 400056, India

Introduction

Solid dispersion (SD) is one of the most effective strategies to improve the dissolution profile and bioavailability of poorly water-soluble drugs [1]. By definition, SDs include those formulations where a drug is dispersed in a matrix preferably some hydrophilic polymer in different states such as eutectic mixtures, crystalline/glass solution, or amorphous suspension [2]. However, amorphous SD (ASD) is the most commonly used SD, where the drugs are dispersed in the polymeric matrix in the amorphous state [1, 3]. ASD usually has the capacity to enhance dissolution because no energy is required to break the crystal structure as the crystalline form is not present [4, 5]. It is anticipated that once an ASD system dissolves, drugs are presented as a super-saturated solution and the precipitated drugs are meta-stable. This meta-stable polymorphs exhibit higher solubility than the most stable crystalline form [3, 6].

The ASD system belongs to a high energy state which is very susceptible to revert into a less energetic crystalline state. During processing and storage, amorphous to crystallization change-over, known as recrystallization, may occur, which compromises the drug dissolution enhancement. [7, 8]. The two most important factors to develop and prepare a stable SD with enhanced dissolution are the selection of a suitable carrier (usually a polymer) and the use of the proper method of preparation. The wise selection of polymer with high T_g , good hydrogen bonding or miscibility with the drug as well as less water absorption is the way of stabilizing ASD [9, 10]. Since earlier days, various polymers are being used as a carrier for ASD; for example, PVP (K12 to K30), HPMC, PEG (1500 to 20,000), poloxamer, and grafted copolymer of polyvinyl caprolactam (Soluplus®) [11, 12]. Combined polymer or a binary composition of polymers such as PVP K 30-PEG or PVP K 30-poloxamer 188 were also incorporated as SD carriers to reduce the melting temperature of the system or to exhibit much higher drug dissolution [9, 13].

SD can be prepared by either thermal process which involves fusion of drug-carrier mixture by heat, or solvent evaporation process which involves the safe and API soluble organic or aqueous vehicle. All these methods have their characteristic advantages and disadvantages [14–18]. Due to various types of stresses imposed on the API and carriers during the preparation of SD by various methods, the characteristics of the products usually become different. These characteristics include the improvement in drug dissolution, drug-polymer interaction, the formation of the amorphous particle, the stability of SD, and bulk density of solid dispersed powder, etc. These properties give a huge impact not only on the performance of the final product but also on the downstream processing. In this perspective, a comparative study among different SD preparation methods will be very useful to select the most suitable method. Few studies have reported different SD methods, but they rarely extended their work to critically analyze the effect of preparation method on drug-polymer interaction, loss of drug crystallinity, or stability of SD products [10, 19]. More specifically, there is no report on the impact of the preparation method on properties of a SD containing a binary carrier system (PVP K30-poloxamer 188) with nisoldipine as an active pharmaceutical ingredient (API).

This research aimed to study the impact of bench scale thermal method and solvent assisted methods on the drug crystallinity loss, drug-carrier interaction, ex vivo intestinal permeation, and stability of solid dispersed nisoldipine formulated as a ternary SD. Previously our research group has developed and optimized solid dispersed nisoldipine (NSD) using PVP K30-poloxamer binary carrier [9]. In the present research, SD of NSD was prepared by hot melt mixing, solvent evaporation by rotary vacuum evaporator, and lyophilization (freeze-drying), for comparative evaluation. All experimental tests in this research were carried

out in triplicates where the results were expressed with mean \pm standard deviation format.

Materials

NSD (purity > 98.5%), a yellow crystalline powder (aqueous solubility 2.27 g/L), was purchased from Hangzhou Hyper Chemicals Ltd., Hangzhou, China. PVP K30 and poloxamer 188 were purchased from Apollo Healthcare Resources, Singapore and Merck KGaA, Germany, respectively. All other reagents and chemicals used for the research were analytical grade and purchased from Permula Chemicals Sdn. Bhd., Malaysia.

Methods

Preparation of Solid Dispersion by Different SD Methods

Solid dispersed NSD was prepared by three different methods: hot melt mixing (HM), rotary evaporation (SE), and freeze-drying (FD). The composition was NSD:PVP K30:poloxamer 188 (1:3.75:6.55) weight ratio, which has been developed and optimized in our previous research [9].

Physical mixture (PM), in the same composition as SD, was prepared by dry mixing of all ingredients.

HM method was prepared by the rapid cooling process where the drug and polymeric carriers are mixed, melted (60 ± 2 °C), stirred, and the mixture was immediately transferred onto an ice bath to solidify followed by overnight air drying, pulverization, and sieving. Henceforth, the SD prepared by HM method will be termed as HMSD.

In SE method, drug and carriers were added into the minimum possible quantity of absolute ethanol and gently heated (40 ± 2 °C) to obtain a clear mixture. Rotary vacuum evaporator (BUCHI R 210, Switzerland) was used to remove the solvent at 60 °C and 175 mbar. Then, SD material was collected, dried, pulverized, and sieved. SD prepared by this method will be denoted as SESD.

For FD method, polymers were dissolved in distilled water and then NSD was added to the solution with constant stirring. The mixture was then freeze-dried at -45 °C and 7×10^{-2} a pressure using Freeze Dryer (Alpha 1–2 LD Plus Christ) for 48 h. SD prepared by FD method will be abbreviated as FDSD.

All prepared SD formulations were sieved through 250 μ m sieve and the undersize fractions were used for further analysis. The percentage yield of the solid dispersed product was calculated in comparison using the following equation,

$$PY = \frac{AY}{TY} \times 100\% \quad (1)$$

Where, PY = percentage yield, AY = actual yield, TY = theoretical yield (cumulative amount of all ingredients).

Saturation Solubility Study

For shake-flask method, an excess amount of sample was added to 10 mL of medium (pH 6.8 phosphate buffer with 0.4% sodium lauryl sulfate/SLS) and shaken for 24 h at 150 RPM, 37 ± 2 °C in an incubator shaker. The absorbance of sample aliquot was measured at 235 nm spectrophotometrically and the concentration of NSD was calculated from a linearity plot to express the saturation solubility.

Scanning Electron Microscopy Study

Scanning electron microscope (Evo 50, Carl Zeiss Microscopy, Jena, Germany) and gold coating with a tabletop sputter coater (Leica EM SCD 005, Leica Microsystems (SEA) Pte. Ltd.) were employed for recording scanning electron microscopy (SEM) micrographs and morphology analysis.

Crystallinity Study by XRD

X-ray powder diffractometer (Rigaku Ultima-IV, Japan) was used to scan the samples from 0° to 70° with 5°/min speed using Cu-K radiation at 40 kV voltage 30 mA current to record diffraction angles (2θ) and intensity (counts).

Drug-Polymer Interaction by Attenuated Total Reflectance Infra-red Spectroscopy

Interactions between NSD and the carriers were studied by attenuated total reflectance infra-red (ATR-IR) spectroscopy (Perkin Elmer, USA). Each sample was clamped on ATR diamond crystal with <90 units force and scanned over 4000–400 cm^{-1} IR ray range for accumulations 15 scans at resolution 2 cm^{-1} .

Thermal Analysis by DSC

Thermograms of samples were derived by a differential scanning calorimeter (1-STARe, Mettler Toledo, Columbus, OH). Each sample (5–10 mg) was enclosed in an aluminum crucible and exposed to a thermal range of 10–200 °C (10 °C/min) under constant nitrogen flow (10–20 mL/min) where an aluminum crucible without sample was used as the blank.

Ex Vivo Permeability Study Through the Intestinal Membrane

The ex vivo study was done as per the methods reported by Dixit et al. (2012). Krebs-Ringer bicarbonate buffer was prepared from 118.0 mM NaCl, 4.7 mM KCl, 2.5 mM CaCl_2 , 1.2 mM $\text{MgSO}_4 \cdot 7 \text{H}_2\text{O}$, 25.0 mM NaHCO_3 , 1.2 mM KH_2PO_4 , and 5.5 mM glucose. Rabbit intestines were donated by a fellow research group of Kulliyyah of Pharmacy, International Islamic University Malaysia (IIUM). The research group obtained the approval for the animal study from the Institutional Animal Care and Use Committee (IACUC) of IIUM, Kuantan, Malaysia (Animal Ethics Approval no: IIUM/IACUC Approval/2016/(9)(54)). Small intestinal parts were cut into 15 cm length, fat removed and rinsed with Krebs's buffer. Each intestine was everted with a tiny glass rod and mounted in a specially designed glass apparatus as described by Dixit et al. with little modification [20]. The inner side of the intestinal tube is perfused with Krebs's solution. Then the glass assembly with 2.3 cm length of the everted intestinal tube is placed in a beaker containing sample 100 $\mu\text{g}/\text{mL}$ with phosphate buffer (pH 6.8) solution. At 15, 30, 45, 60, and 120 min time points, samples were collected from the everted intestinal sac and analyzed by a simple reversed-phase high performance liquid chromatography (HPLC) method at 235 nm. The HPLC method used an Agilent Zorbax C18 column (250 mm \times 4.6 μm) acetonitrile-water (1:1 v/v) mobile phase at 1 mL/min flow rate. The run time was 11 min and NSD was detected at 8.78 min by a sharp peak without any significant interference. HMSD, SEFD, FDS, and raw NSD were used as samples for the study. The concentration of permeated drug was calculated from the area of generated NSD peak in the chromatogram through the linearity curve equation. The apparent permeability coefficient (P_{app}) was calculated using the following equation [20]:

$$P_{\text{app}} = \frac{dQ}{dt} * \frac{1}{A * C_0} = V * dt * A * C_0 \quad (2)$$

Where, P_{app} = apparent permeability coefficient, dQ/dt = the cumulative amount of drug (Q) appearing in the acceptor (serosal) compartment as a function of time, A = surface area of the intestine (cm^2), C_0 = the initial concentration of drug in the donor compartment ($\mu\text{g}/\text{mL}$), V = volume of sample (mL).

Stability Study

Both the real-time and accelerated stability studies were carried out for 3 months. HMSD, SESD, FDS, and PM materials were packed in separate sealed plastic bags, wrapped with aluminum foil, and placed in real-time stability chamber

(30 °C/75% RH) as well as in accelerated stability chamber (40 °C/75% RH). The samples were analyzed at 1 week, 2 weeks, 1 month, 2 months, and 3 months of sampling points. At each sampling point, physical observation for the change of color or formation of lump, saturation solubility study, and ATR spectroscopy were carried out.

Results and Discussion

Percentage Yield of Solid Dispersed NSD Prepared by Different Methods

Percentage yield represents the recovery of solid dispersed NSD from the apparatus used during formulation. FD method showed the highest percentage ($97.68 \pm 2.2\%$) followed by HM ($95.45 \pm 3.5\%$) and SE ($84.53 \pm 6.2\%$) method. FD product was easily recovered from the container and HMSD materials were relatively harder while the SE method imposed the maximum loss of materials during collection from rotatory evaporator flask. Every single method employed in this study has its own pros and cons [1]. Easy and maximum yield from a process is industrial desirability.

Comparison of Saturation Solubility Among HMSD, SESD, and FDSD

NSD has very limited solubility in water ($2.27 \pm 0.15 \mu\text{g/mL}$) or in 0.1 N HCl acidic condition ($1.22 \pm 0.0142 \mu\text{g/mL}$), as observed in the preliminary study. Therefore, pH 6.8 phosphate buffer with 0.4% SLS was chosen as a solubility medium representing the intestinal fluid. The solubility results of raw NSD, SESD, HMSD, and FDSD were 63.33 ± 0.32 , 111.85 ± 2.25 , 117.41 ± 2.21 , and $123.89 \pm 6.11 \mu\text{g/mL}$ respectively. All solid dispersed NSD showed statistically significant improvement of NSD solubility compared to the pure drug with p value < 0.05 at 95% confidence interval. No statistically significant difference was seen among three SD formulations although FDSD showed maximum solubility followed by SESD and HMSD. When a solid dispersed formulation encounters an aqueous medium, hydrophilic carriers and dispersed drug become wet and partly soluble. Several factors are involved behind this phenomenon such as the formation of high surface area, increased wettability, and increased porosity of solid dispersed powder [21]. As the compositions of all formulations were the same, the difference in solubility could be due to the degree of drug crystallinity and the physical nature of the powder (porosity). For FDSD, the porosity was significantly higher compared to HMSD and SESD. Freeze-drying forms amorphous product with high porosity due to the removal of water by sublimation. The porosity values calculated based on total volume and void volume of FDSD, HMSD, and SESD were

$17.25 \pm 1.99\%$, $12.43 \pm 2.09\%$, and $12.05 \pm 1.57\%$, respectively. All samples were broken down into smaller fragments within 8 h during the solubility study. Therefore, no significant difference in saturation solubility was seen although there was a difference in porosity values. Other responsible factors of solubility have been critically studied by SEM, DSC, ATR, or XRD analysis as described in the subsequent sections.

Morphological Comparison Among HMSD, SESD, and FDSD

The shape and surface morphology of sample particles were examined by SEM. NSD appeared as elongated irregular crystals, whereas PVP K30 and poloxamer 188 both were round-shaped particles (Fig. 1). In HMSD and SESD images, irregularly shaped less porous solid dispersed materials were sighted without clearly distinguishable NSD crystals (Fig. 1). The non-visibility of NSD

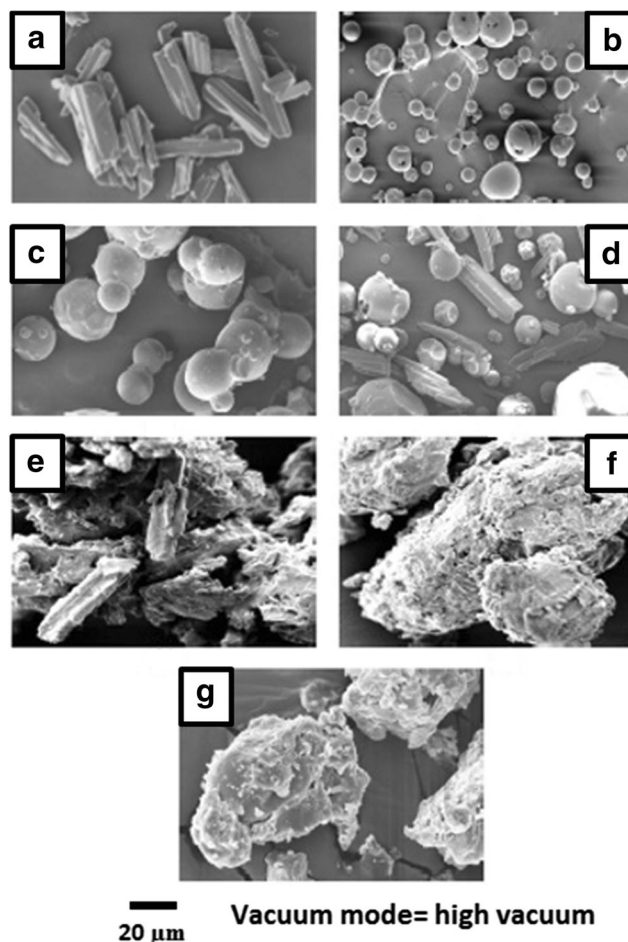


Fig. 1 Scanning electron microscopy images. Nisoldipine (a). PVP K30 (b). Poloxamer 188 (c). Physical mixture (d). FDSD/freeze-dried solid dispersion (e). HMSD/melt mixed solid dispersion (f). SESD/rotary vacuum evaporated solid dispersion (g). Magnifications taken were $\times 32$ (c, d) and $\times 465$ (rest of the images)

crystals in HMSD and SEDS may confer the loss of NSD crystallinity during SD process. In contrast, NSD crystals were sighted in FDS image because the hydrophobic nature of NSD caused partial retaining of drug crystallinity since FD process involved water as the solvent. During the pre-freezing part of FD process, some NSD crystals settled down at the bottom of the beaker which did not turn into an amorphous form. However, a SD system can be either a crystalline or amorphous drug or a mixed form of the drug, dispersed in the amorphous or crystalline carrier [22]. In this case, based on SEM image, primarily it can be said that FD method could not produce SD with complete NSD amorphization although it showed a more porous surface which gave the advantage of faster and higher dissolution compared to the other two SDs.

Effect of Method of Preparation on Drug-Carrier Interaction

The infra-red spectroscopy technique analyzes the interaction between different functional groups. The IR spectrum (Fig. 2) of NSD showed a characteristic peak at $3320.6 \pm 0.69 \text{ cm}^{-1}$ which was accountable for N-H stretching of dihydropyridine (DHP) ring. The wide band between 2800 to 3100 cm^{-1} and two strong peaks at $1705.17 \pm 0.18 \text{ cm}^{-1}$ and $1649.78 \pm 0.67 \text{ cm}^{-1}$ were attributed to the aliphatic C-H bonds and the stretching of two carbonyl (C=O) groups present in the side chain of DHP moiety, respectively. NO_2 stretching generated two bands, at $1529.98 \pm 0.88 \text{ cm}^{-1}$ and $1347.18 \pm 0.13 \text{ cm}^{-1}$. At $1490.85 \pm 0.47 \text{ cm}^{-1}$ and $1211.24 \pm 0.05 \text{ cm}^{-1}$, peak for aromatic C=C stretching and C-O stretching was observed, respectively. All the characteristic peaks found in NSD IR spectrum were in close agreement with previous literature [23]. In PVP K30, a number of vibrational bands have been identified, such as $1647.73 \pm 0.87 \text{ cm}^{-1}$ (C=O stretching of carboxylic acid), $2948.83 \pm 0.71 \text{ cm}^{-1}$ (C-H stretching), and $3250\text{--}3600 \text{ cm}^{-1}$ (O-H stretching), which were broadened due to absorbed moisture. For poloxamer 188, characteristic peaks that were visible in the IR spectrum include $1099.45 \pm 0.54 \text{ cm}^{-1}$ (C-O stretching), $1341.66 \pm 0.91 \text{ cm}^{-1}$ (O-H bend-

ing), and $2800\text{--}3100 \text{ cm}^{-1}$ with a peak at $2876.86 \pm 0.32 \text{ cm}^{-1}$ (C-H vibration). These peaks obtained for the two carriers were also in-line with other published reports [24, 25].

In PM, all characteristic peaks of NSD were observed with C-H stretching band overlapping at $2800\text{--}3100 \text{ cm}^{-1}$. No interaction was observed between the drug and carriers in dry state. Clear differences were observed among the IR spectrums of HMSD, SEDS, and FDS (Fig. 2). The N-H vibrational peak position at 3320.6 cm^{-1} was shifted towards lower wavenumber with reduced intensity in the ascending order of $\text{SESD} < \text{HMSD} < \text{FDS}$. This case represented a reduction in drug crystallinity [26]. In FDS, that peak was almost absent or masked by a wide band of excess moisture in the sample. The more porous nature of the FDS material could be the reason for higher hygroscopicity. There were previous reports on shift or absence of N-H stretching peak in the amorphous form of an anti-inflammatory drug (nifedipine) containing an amino group where the amine stretching vibration band of amine and carbonyl groups were broadened and less defined [27, 28]. In this research, the same type of interactions has been observed but to different degrees depending on the method of preparations. Another reason for the absence of N-H band in FDS might be H bonding. Not only N-H band, but the C=O vibrational peak at 1705.17 cm^{-1} was also not observed in FDS. The same peak was observed with lower intensity in SEDS followed by HMSD. From the structure of NSD [29], two H bonding sites are presented in the molecule: proton donor amine (-NH) group and proton acceptor carboxylic (C=O) group. These groups can form H bonding with PVP K30 and hydroxyl group of poloxamer 188. A report on nifedipine amorphous particles also showed a carbonyl stretching band at 1705 cm^{-1} , which was responsible for H bonding with the polymer [28]. H bonding between drug and polymer helps in reduction of molecular mobility in the SD products to retain the amorphous structure of the drug.

A strong band of C=C aromatic stretching (1491.70 cm^{-1}) presented in raw NSD had shifted a bit towards higher wavenumber ($1493.70 \pm 0.41 \text{ cm}^{-1}$) for SEDS and HMSD while it

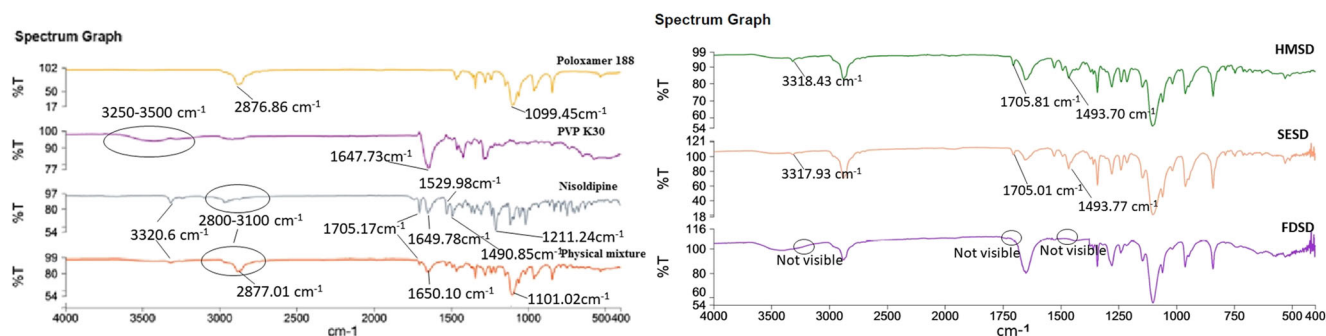


Fig. 2 Infra-red spectrums of solid dispersed samples produced by freeze-drying (FDS), melt mixing (HMSD), and rotary vacuum evaporating (SESD)

was absent for FDSD. Significant differences were also observed in two other fingerprint IR peaks of NSD: C-O stretching of carboxylate group at 1211.24 cm^{-1} and 1101.52 cm^{-1} . The first peak was not well defined in FDSD (1211.29 cm^{-1}), whereas it was shifted to $1213.7 \pm 0.49\text{ cm}^{-1}$ and 1213.51 cm^{-1} in HMSD and SESD spectrums. In SESD and FDSD, the vibration band was present at 1101.52 cm^{-1} while little shift was seen in HMSD spectrum (1103.8 cm^{-1}). Peak shifts occur due to many reasons such as the formation of new bonding, change in crystallinity, and change in concentration in the sample [27]. From these drug-polymer interaction studies, the highest degree of H bond formation between NSD and both carriers (PLX 188 & PVP K30) was observed in FDSD compared to the other two methods. The loss of NSD crystallinity was also noted here where PXRD and DSC studies were continued to analyze it further.

Effect of Method of Preparation on Drug Crystallinity

PXRD is a valuable tool to identify and analyze the crystallinity of a material. The sharp characteristic peaks at 2θ angle of 9.30° , 9.79° , 11.30° , 12.46° , 19.00° , 22.76° , 25.34° , 26.14° , and 27.48° (Fig. 3) clearly indicated that NSD exists as crystals [30, 31].

The discussion to critically evaluate the loss of drug crystallinity was extended by calculating the relative intensity instead of absolute intensity because it is not varying with instrumental and analysis conditions. Peak area value was used after baseline correction instead of peak height because it is more precise to calculate peak intensity [32]. The relative intensity of the peaks at 2θ angles of 9.30° , 9.79° , 11.30° , 19.00° , 22.76° , and

Table 1 Relative intensities of peaks in X-ray diffractogram at selected 2θ angle

2θ angle	Relative intensity (%)			
	NSD	SESD	HMSD	FDSD
9.30	61.1	5.2	11.3	11.2
9.79	90.3	X	11.6	11.8
11.30	69.1	3.7	11.1	5.1
12.46	17.3	X	X	X
19.00	100	X	X	X
22.76	72.4	100	100	100
27.48	31.3	X	7.3	4.6

NSD, raw nisoldipine; SESD, solid dispersion prepared by solvent evaporation; HMSD, solid dispersion prepared by hot melt mixing; FDSD, solid dispersion prepared by freeze-drying; “X” indicates no peak

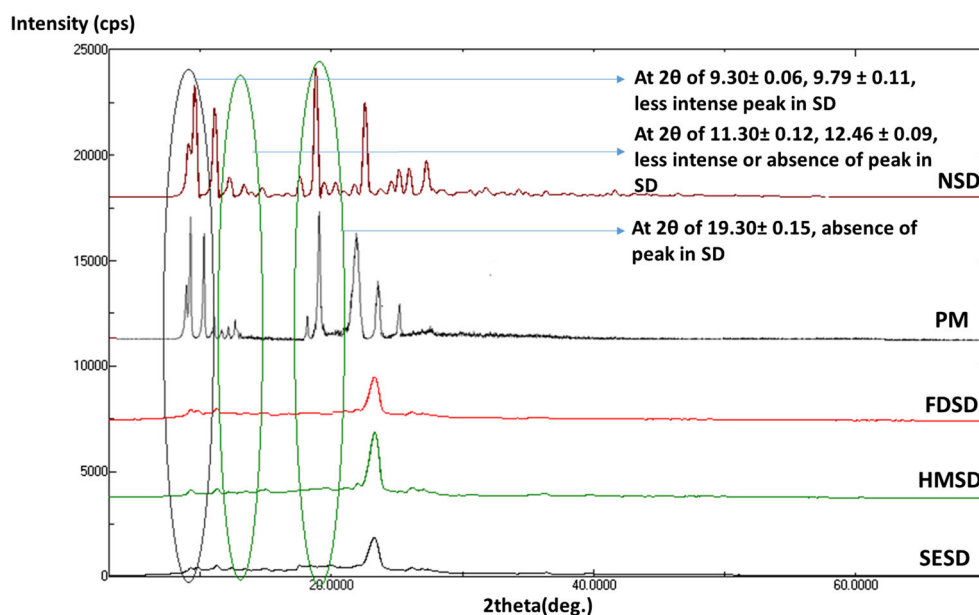
27.48° was calculated based on the following equation and the results were presented in Table 1:

Relative intensity

$$= \frac{\text{Absolute intensity}}{\text{Intensity of the most intense peak}} \times 100\% \quad (3)$$

The 2θ values were chosen from the diffractogram of raw NSD based on the considerably higher area and as mentioned in other literature [30, 31]. In PM, all NSD characteristic peaks were present with comparable relative intensity as pure NSD indicating the presence of NSD crystal in the dry mixture. On the other hand, loss of NSD crystallinity was observed in all three SD types where the relative intensities of some peaks (9.30° and

Fig. 3 Powder X-ray diffractograms of solid dispersed samples produced by freeze-drying (FDSD), melt mixing (HMSD), and rotary vacuum evaporating (SESD)



11.30°) were decreased and some (12.46° and 19.00°) were not defined. The absence or reduction in XRD peak intensity indicates loss or reduction of drug crystallinity. Drug particles in the amorphous phase can be dissolved more rapidly than fully crystalline drugs and enhance drug dissolution [33]. In this research, the improved aqueous solubility of NSD was successfully achieved by SD techniques, behind which reduction or loss of NSD crystallinity was the main factor although it was not complete conversion to amorphous form.

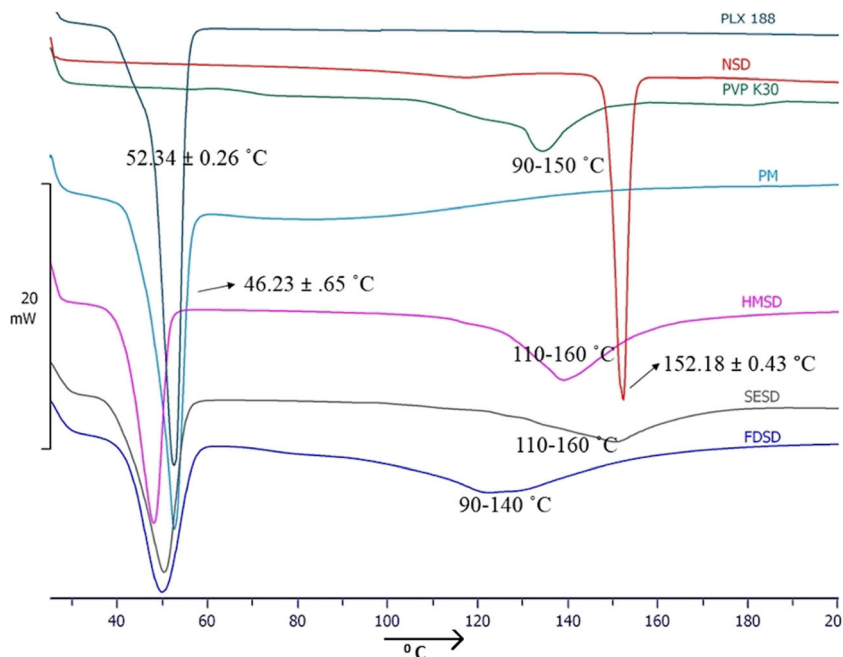
The intensity of NSD crystallinity loss among three different methods could be compared as SESD>FDSD>HMSD. As shown in Table 1, the relative intensity of SESD at 11.30° peak was 3.70%, followed by FDSD (5.1%) and HMSD (11.1%). SESD had the highest loss of NSD crystallinity compared to the other SD methods. During the initial stage of SESD preparation, the drug was completely dissolved in the organic solvent which caused finer dispersion inside the polymeric matrix and resulted in significant loss of crystallinity after the solvent evaporated. In the freeze-drying method, hydrophobicity of NSD to the aqueous solvent and the residue of moisture initiated the recrystallization process which resulted in traces of crystallinity [18, 34]. Compared to the other two methods, HMSD was the easiest to prepare. However, heat stress was given during the dispersion followed by rapid quenching. Such rapid cooling can convert some amount of the dissolved drug to finer crystals instead of amorphous form led to having higher diffraction intensities compared to the other two methods [35, 36].

Thermal Analysis by DSC

The thermal behavior of a sample can reveal an idea about the crystallinity and glass transition of a SD system. The DSC thermograms were presented in Fig. 4. Raw NSD exhibited a sharp endothermic peak at 152.18 ± 0.43 °C with the enthalpy of 142.68 ± 2.3 J/g, confirming the crystalline state [30]. PVP K30 produced a broad endothermic band from 90 to 150 °C due to the release of the absorbed moisture, which was also evidenced by ATR studies [25]. Poloxamer 188 showed a melting endotherm at 52.34 ± 0.26 °C. In PM, a sharp peak was observed at 46.23 ± 0.65 °C with a broad endotherm at 100–140 °C but no sharp melting peak of the drug. Absence or shifting of drug peak towards a lower value may indicate possible interaction between drug and polymeric carriers. However interaction was not possible for a physical mixture, rather a eutectic mixture could be formed in the DSC crucible due to the low melting point of poloxamer 188 and complete miscibility of NSD in the molten polymer during the analysis. Therefore, no NSD peak was visible in the PM [37]. Tang et al. (2018) explained that febusostat formed eutectic mixtures during melting with poloxamer 188 and PVP K30 in a ternary system [25]. NSD crystals were completely miscible with molten PVP K30 resulting in a broad transition band because the transition of PVP K30 occurs at a lower temperature than the melting point of NSD.

In the thermograms of all three SDs, no NSD peak was observed, which could be due to the drug solubilization in molten polymer, the formation of a molecular level dispersion, or drug distribution in an amorphous state in the SD [38]. These results also indicated the significant reduction of NSD

Fig. 4 DSC thermograms of poloxamer 188 (PLX), nisoldipine (NSD), PVP K30 and solid dispersed samples produced by freeze-drying (FDSD), melt mixing (HMSD), and rotary vacuum evaporating (SESD)



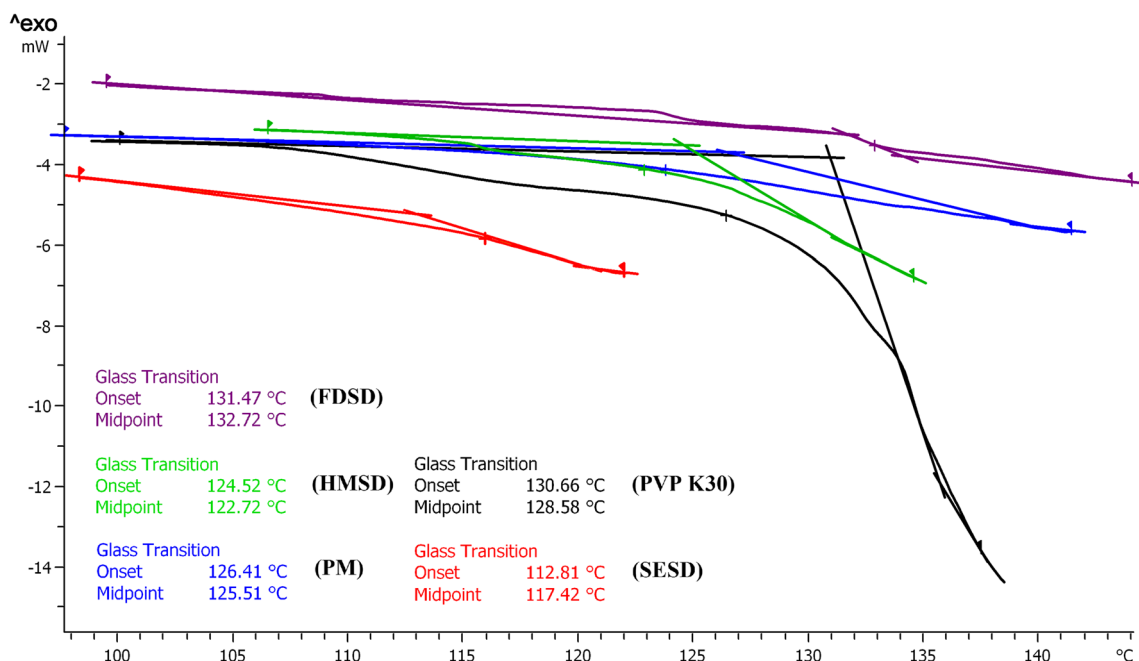


Fig. 5 T_g of physical mixture (PM), PVP K-30, and solid dispersed samples produced by freeze-drying (FDSD), melt mixing (HMSD), and rotary vacuum evaporating (SESD)

crystallinity after employing SD methods. All three SDs thermograms had an endothermic peak at 50 °C or below due to the poloxamer 188 crystals (Fig. 4) where the enthalpy values of the peaks were not statistically different. Overlapping three thermograms of SDs showed a broad endothermic region within the range of 100–160 °C, possibly due to the glass transition of amorphous PVP K30 and evaporation of its associated moisture. Based on the results, the developed SDs can be reported as a two-phase system: crystalline poloxamer 188 and amorphous NSD mixture in PVP K30. A ternary SD containing poloxamer 188 and PVP K30 with aripiprazole two-phase system was reported in the SD prepared by hot melt extrusion process [39]. Moreover, the position of the glass transition band was also analyzed where the enthalpy values of the band for HMSD were significantly higher than SESD and FDSD. As mentioned before, for HM method, the melted drug and polymeric carriers would be finely dispersed at eutectic composition but the drug could crystallize back by rapid

cooling [35, 36]. Those NSD crystals in HMSD, although in considerably low concentration, melted along with PVP K30 during DSC analysis and the enthalpy of the band at 100–160 °C was increased significantly (relatively higher crystallinity) than SESD or FDSD.

In all SDs, the mid-point of glass transition (Fig. 5) varied but the difference was not significant (p value > 0.05, at 95% confidence interval). Pure PVP K30 and physical mixture resulted in T_g of 128.58 °C and 125.51 °C, respectively, which showed no significant difference. Similarly, the T_g for three different SDs was also statistically the same as the PVP K30 or PM. These results indicated that the amorphous state of PVP K30 was maintained in the SDs, and NSD was dispersed at the molecular level or in the fine crystalline state throughout the hydrophilic carrier. The T_g of the SD system was higher than normal storage temperature, indicating a lesser chance of recrystallization of amorphous drug particles in SD samples during storage [40].

Fig. 6 **a** Permeability P_{app} (cm/s) of drug for different SD formulations. **b** %CDP at 2 h for solid dispersed samples produced by freeze-drying (FDSD), melt mixing (HMSD), and rotary vacuum evaporating (SESD)

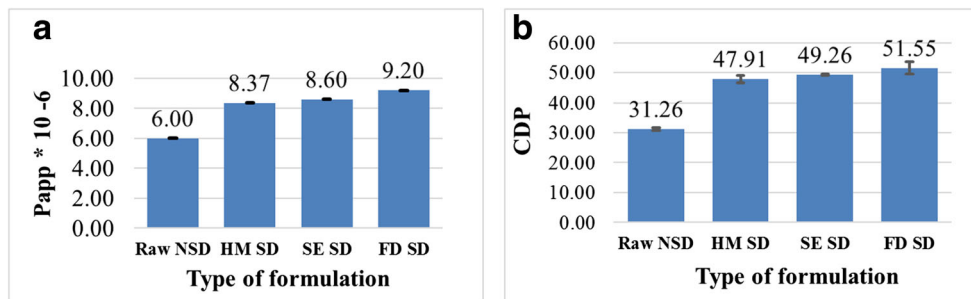


Table 2 Physical observation of all SD stored in different storage conditions

Time points	PM		HM		SE		FD	
	RT	AC	RT	AC	RT	AC	RT	AC
0 day	S	S	S	S	S	S	S	S
1 week	S	NS	S	S	S	S	S	S
2 weeks	NS		S	S	S	S	S	NS
1 month			S	S	S	NS	S	
2 months			S	NS	S		NS	
3 months			S		S			

RT, real-time stability condition; AC, accelerated stability condition; S, stable (segregated dry powder); NS, not stable (agglomerated moist mass)

Ex Vivo Permeability Comparison Among HMSD, SESD, and FSD

For BCS class II drugs, the presence of excipients and modified formulation can effectively enhance drug solubility and permeability, which can be studied by ex vivo intestinal permeation [41]. The apparent permeability (P_{app}) and percentage cumulative drug permeated (%CDP) through rabbit intestinal mucosa were evaluated by ex vivo permeation (Fig. 6).

From the results depicted by Fig. 6a, it was observed that all three SDs showed significantly higher permeability (P_{app}) as well as higher %CDP compared to raw NSD. The P_{app} of NSD through rabbit intestinal mucosa was $6.04 \times 10^{-6} \pm 8.78 \times 10^{-8}$ cm/s. At 2 h, only $31.26 \pm 0.47\%$ drug was permeated cumulatively through the membrane which was significantly lower than all three SDs. Although there are no strict cut-off values of permeability for different BCS class of drugs, as per some literature, BCS II drugs should fall under P_{app}

value $> 10^{-5}$ cm/s through Caco-2 cell layer [42]. In the same literature, a borderline class was mentioned with P_{app} value between 2×10^{-6} and 10^{-5} cm/s. In this study, raw NSD stood under this borderline range representing poor permeability. If the solubility of the drug could be enhanced, the permeability would be also improved. Since the result of the solubility study showed significant improvement of NSD solubility in the small intestinal medium by SD formulations, their ex vivo intestinal permeability showed higher results as well.

The presence of polymers (poloxamer 188 or PVP K30) could alter the membrane fluidity and cause improved drug permeation through the intestinal mucosal wall. If the permeability followed that rule, all three SD formulation should give the same P_{app} result. However, a statistically significant difference (p value < 0.05) in the P_{app} result was observed among the three SD samples. Hence, the effect of polymers on intestinal permeability can be considered as negligible. The difference in permeability was due to the difference in solubility resulted from the difference in SD methods. Like the saturation solubility study, ex vivo permeation of FSD showed the highest P_{app} compared to HMSD and SESD.

Percent CDP at 2 h did not show a statistically significant difference among different SDs (Fig. 6b). FSD result was numerically higher from the initial point of sampling (more than 3% at 15 min) compared to HMSD and SESD (near to 1% at 15 min). Both %CDP and P_{app} results clearly indicated that the method of SD preparation had a significant impact on intestinal drug permeation and absorption. There is no report published on intestinal permeation of NSD yet, but another drug of the same class (Dihydropyridine) was reported that improvement of solubility affected intestinal permeability positively [43, 44].

Fig. 7 **a** Infra-red spectrums of all SD formulations at 2 months stored in real-time stability chamber. **b** Infra-red spectrums of all SD formulations at 2 months stored in accelerated stability chamber. Two months' time point has been presented due to significant changes at this point. FSD: freeze-dried solid dispersion, HMSD: melt mixed solid dispersion, SESD: rotary vacuum evaporated solid dispersion

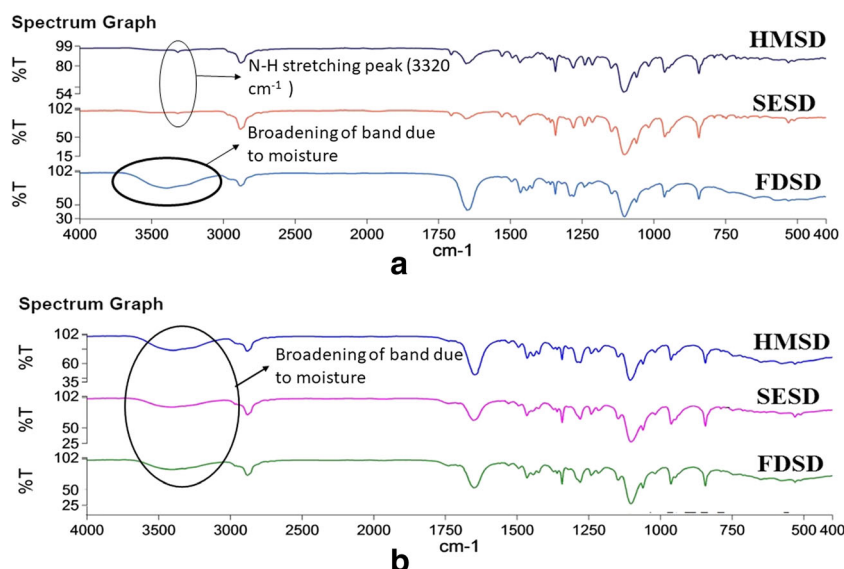
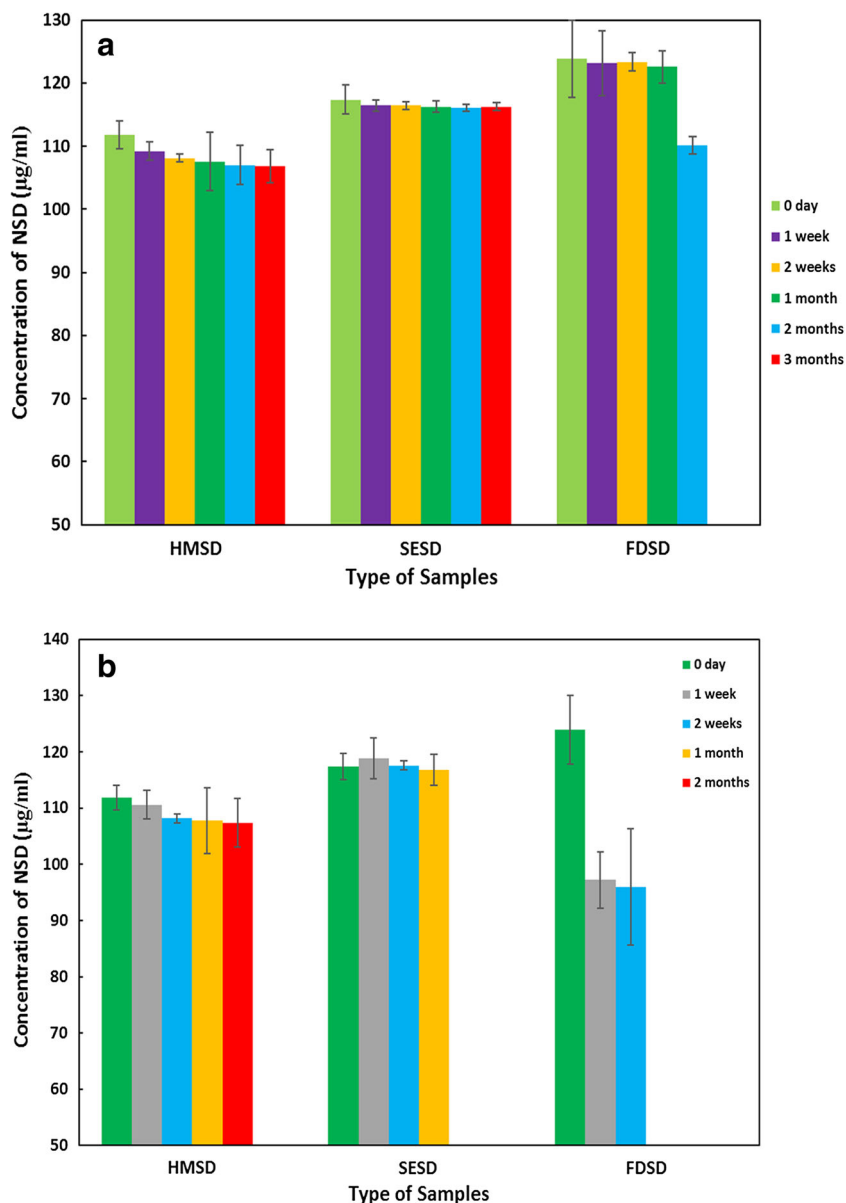


Fig. 8 **a** Saturation solubility results of SD formulations stored under real-time stability condition. **b** Saturation solubility results of SD formulations stored under accelerated stability condition. The stability studies were discontinued at the time points where the SD became completely moist mass. FDSD: freeze-dried solid dispersion, HMSD: melt mixed solid dispersion, SESD: rotary vacuum evaporated solid dispersion



Effect of Storage Condition on Stability of SD Prepared by Different Methods

The stability of SD materials was studied for 3 months and visual observations were recorded (Table 2). In accelerated condition, all three SD powders became moist mass at 2 months or before. In real-time conditions, only FDSD powder became moist at 2 months, whereas HMSD and SESD powder retained their dry nature for up to 3 months. Visually all SD powders were highly susceptible to moisture absorption, possibly due to the presence of hydrophilic ingredients. FDSD powder had a lower bulk density (0.27 ± 0.003 g/mL, Data not shown) compared to HMSD and SESD powder, indicating the loose powder mass which could naturally

absorb the highest moisture. Another reason could be the presence of excess moisture residue in FDSD as quite a high amount of water was involved in the preparation.

The ATR spectrum of different SDs (Fig. 7) from the stability samples showed a clear presence of moisture with broadening of the IR band at $3100\text{--}3500$ cm^{-1} . The broadening of this band was the maximum in the case of FDSD at 2 weeks of accelerated storage condition. The moisture indicating IR band is rather not visible in HMSD or SESD sample stored in real-time condition. Moreover, the identified N-H vibration of NSD at 3320 cm^{-1} was either absent or suppressed by increased moisture in all accelerated storage samples at 2 weeks or later.

The absorbed moisture could be highly detrimental to drug stability as well as to the amorphous state of drugs. The T_g of water is $-137\text{ }^\circ\text{C}$, which can lower down the T_g of the system and in turn increase the molecular mobility [45]. Increased molecular mobility initiates recrystallization and thereby improvement of solubility might be compromised over storage time. Not only that, but water can also disrupt drug-polymer interaction by competitively forming more hydrogen bonding with hydrophilic polymers replacing drug-polymer bonds [45, 46]. From the results of this study, different SD methods were seen to have different degrees of moisture adsorption nature.

The results of the saturation solubility of NSD from different SD at various time points are presented in Fig. 8. In the case of HMSD and SESD, there was no statistically significant difference (p value > 0.05 at 95% confidence interval) in NSD solubility during storage. But in FSDS, in accelerated storage condition, NSD solubility was reduced over time starting from 1 week. We assumed that the higher absorbed moisture in FSDS can cause higher drug recrystallinity which resulted in reduced solubility and stability. The physical nature of the SD materials after the stability sampling points was unacceptable for downstream processing. Considering this level of acceptance, the FD method was the least acceptable and HM was the best out of these three. A more critical investigation on the change of crystallinity was required at each time point of storage to understand and compare the specific effect of moisture on different SDs. There was no previous report on the comparison of storage conditions among different SD preparation methods. Hence, these stability study results will be very beneficial in providing knowledge for better consideration of the preliminary selection of the method of preparation of SD.

Conclusion

A SD of NSD in a fixed combination of binary carrier system containing PVP K30 and poloxamer 188 was prepared by three different lab-scale methods. All three SD such as FSDS, HMSD, and SESD produced a mixed amorphous-crystalline system with significantly improved solubility as well as ex vivo permeation through excised gut mucosa. Freeze-drying had produced the formulation with the highest solubility and ex vivo permeability but poor physical stability during storage. Different degrees of drug-polymer interaction, mostly by H bonding, were observed which varied with the method of preparation. Loss of crystallinity was the highest in SESD, followed by FSDS. For PVP K30-poloxamer 188 binary carrier system for NSD, freeze-drying could be the best method, if not long-term storage of the solid dispersed powder is required. Otherwise, hot melt mixing is the best alternative in terms of stability and downstream processing.

Acknowledgments The authors would like to acknowledge the financial support from Research Management Centre, International Islamic University Malaysia (IIUM) for supporting the research through the “Endowment grant” (EDW B 14-097-0982).

Compliance with Ethical Standards

Conflict of Interest The authors declare that they have no conflict of interest.

References

1. Vo CLN, Park C, Lee BJ. Current trends and future perspectives of solid dispersions containing poorly water-soluble drugs. *Eur J Pharm Biopharm.* 2013;85:799–813.
2. Chiou WL, Riegelman S. Pharmaceutical applications of solid dispersion systems. *J Pharm Sci.* 1971;60:1281–302.
3. Huang Y, Dai WG. Fundamental aspects of solid dispersion technology for poorly soluble drugs. *Acta Pharm Sin B.* 2014;4:18–25.
4. Khadka P, Ro J, Kim H, Kim I, Kim JT, Kim H, et al. Pharmaceutical particle technologies: an approach to improve drug solubility, dissolution and bioavailability. *Asian J Pharm Sci.* 2014;9:304–16.
5. Lust A, Strachan CJ, Veski P, Aaltonen J, Heinamaki J, Yliruusi J, et al. Amorphous solid dispersions of piroxicam and Soluplus®: qualitative and quantitative analysis of piroxicam recrystallization during storage. *Int J Pharm.* 2015;486:306–14.
6. Censi R, Martino PD. Polymorph impact on the bioavailability and stability of poorly soluble drugs. *Molecules.* 2015;20:18759–76.
7. Jijun F, Lishuang X, Xiaoguang T, Min S, Mingming Z, Haibing H, et al. The inhibition effect of high storage temperature on the recrystallization rate during dissolution of nimodipine-kollidon VA64 solid dispersions (NM-SD) prepared by hot-melt extrusion. *J Pharm Sci.* 2011;100:1643–7.
8. Feng X, Vo A, Patil H, Tiwari RV, Alshetali AS, Pimparade MB, et al. The effects of polymer carrier, hot melt extrusion process and downstream processing parameters on the moisture sorption properties of amorphous solid dispersions. *J Pharm Pharmacol.* 2016;68:692–704.
9. Oo MK, Mandal UK, Chatterjee B. Polymeric behavior evaluation of PVP K30-poloxamer binary carrier for solid dispersed nisoldipine by experimental design. *Pharm Dev Technol.* 2017;22:2–12.
10. Bennett RC, Brough C, Miller DA, O'Donnell KP, Keen JM, Hughey JR, et al. Preparation of amorphous solid dispersions by rotary evaporation and kinetisol dispersing: approaches to enhance solubility of a poorly water-soluble gum extract. *Drug Dev Ind Pharm.* 2015;41:382–97.
11. Karavas E, Georarakis E, Sigalas MP, Avgoustakis K, Bikiaris D. Investigation of the release mechanism of a sparingly water-soluble drug from solid dispersions in hydrophilic carriers based on physical state of drug, particle size distribution and drug-polymer interactions. *Eur J Pharm Biopharm.* 2007;66:334–47.
12. Fule R, Amin P. Development and evaluation of lafutidine solid dispersion via hot melt extrusion: investigating drug-polymer miscibility with advanced characterisation. *Asian J Pharm Sci.* 2014;9:92–106.
13. Liu J, Cao F, Zhang C, Ping Q. Use of polymer combinations in the preparation of solid dispersions of a thermally unstable drug by hot-melt extrusion. *Acta Pharm Sin B.* 2013;3:263–72.
14. Serajuddin ATM. Solid dispersion of poorly water-soluble drugs: early promises, subsequent problems, and recent breakthroughs. *J Pharm Sci.* 1999;88:1058–66.

15. Shamma RN, Basha M. Soluplus: a novel polymeric solubilizer for optimization of carvedilol solid dispersions: formulation design and effect of method of preparation. *Powder Technol.* 2013;237:406–14.
16. Singh A, Mooter GVD. Spray drying formulation of amorphous solid dispersions. *Adv Drug Deliv Rev.* 2016;100:27–50.
17. Wikene KO, Hegge AB, Bruzell E, Tonnesen HH. Formulation and characterization of lyophilized curcumin solid dispersions for antimicrobial photodynamic therapy (aPDT): studies on curcumin and curcuminoids LII. *Drug Dev Ind Pharm.* 2015;41:969–77.
18. Frizon F, Eloy JDO, Donaduzzi CM, Mitsui ML, Marchetti JM. Dissolution rate enhancement of loratadine in polyvinylpyrrolidone K-30 solid dispersions by solvent methods. *Powder Technol.* 2013;235:532–9.
19. Chiang PC, Cui Y, Ran Y, Lubach J, Chou KJ, Bao L, et al. *In vitro* and *in vivo* evaluation of amorphous solid dispersions generated by different bench-scale processes, using griseofulvin as a model compound. *AAPS J.* 2013;15:608–17.
20. Dixit P, Jain DK, Dumbwani J. Standardization of an *ex vivo* method for determination of intestinal permeability of drugs using everted rat intestine apparatus. *J Pharmacol Toxicol Methods.* 2012;65:13–7.
21. Vasconcelos T, Sarmiento B, Costa P. Solid dispersions as strategy to improve oral bioavailability of poor water soluble drugs. *Drug Discov Today.* 2007;12:1068–75.
22. Meng F, Gala U, Chauhan H. Classification of solid dispersions: correlation to (i) stability and solubility (ii) preparation and characterization techniques. *Drug Dev Ind Pharm.* 2015;41:1401–15.
23. El-Maghraby GM, Elsergany RN. Fast disintegrating tablets of nisoldipine for intra-oral administration. *Pharm Dev Technol.* 2014;19:641–50.
24. Alhayali A, Tavellin S, Velaga S. Dissolution and precipitation behavior of ternary solid dispersions of ezetimibe in biorelevant media. *Drug Dev Ind Pharm.* 2017;43:79–88.
25. Tang J, Bao J, Shi X, Sheng X, Su W. Preparation, optimisation, and *in vitro-in vivo* evaluation of febuxostat ternary solid dispersion. *J Microencapsul.* 2018:1–13.
26. Barmpalexis P, Koutsidis I, Karavas E, Louka D, Papadimitriou SA, Bikiaris DN. Development of PVP/PEG mixtures as appropriate carriers for the preparation of drug solid dispersions by melt mixing technique and optimization of dissolution using artificial neural networks. *Eur J Pharm Biopharm.* 2013;85:1219–31.
27. Kaushal AM, Chakraborti AK, Bansal AK. FTIR studies on differential intermolecular association in crystalline and amorphous states of structurally related non-steroidal anti-inflammatory drugs. *Mol Pharm.* 2008;5:937–45.
28. Huang J, Wigent RJ, Schwartz JB. Drug-polymer interaction and its significance on the physical stability of nifedipine amorphous dispersion in microparticles of an ammonio methacrylate copolymer and ethylcellulose binary blend. *J Pharm Sci.* 2008;97:251–62.
29. National Center for Biotechnology Information. Nisoldipine. In: PubChem Compound Database. 2005. <https://pubchem.ncbi.nlm.nih.gov/compound/Nisoldipine>. Accessed 22 Oct 2018.
30. Fu Q, Fang M, Hou Y, Yang W, Shao J, Guo M, et al. A physically stabilized amorphous solid dispersion of nisoldipine obtained by hot melt extrusion. *Powder Technol.* 2016;301:342–8.
31. Dudhipala N, Veerabrahma K. Pharmacokinetic and pharmacodynamic studies of nisoldipine-loaded solid lipid nanoparticles developed by central composite design. *Drug Dev Ind Pharm.* 2015:1–10.
32. Speakman SA. Introduction to X-ray powder diffraction data analysis. Massachusetts Institute of Technology <http://prism.mit.edu/xray/introductiontoxrpddataanalysis.pdf>. Accessed 22 Oct 2018.
33. Alagdar GSA, Oo MK, Sengupta P, Mandal UK, Juliana MJ, Chatterjee B. Development of a binary carrier system consisting polyethylene glycol 4000-ethyl cellulose for ibuprofen solid dispersion. *Int J Pharm Investig.* 2017;7:142–8.
34. Howlader SI, Chakrabarty JK, Faisal KS, Kumar U, Sarkar MR, Khan MF. Enhancing dissolution profile of diazepam using hydrophilic polymers by solid dispersion technique. *Int Curr Pharm J.* 2012;1:423–30.
35. Haleblan J, McCrone W. Pharmaceutical sciences pharmaceutical applications of solid. *J Pharm Sci.* 1969;58:911–29.
36. Ngo AN, Thomas D, Murowchick J, Ayon NJ, Jaiswal A, Youan BBC. Engineering fast dissolving sodium acetate mediated crystalline solid dispersion of docetaxel. *Int J Pharm.* 2018;545:329–41.
37. Newa M, Bhandari KH, Oh DH, Kim YR, Sung JH, Kim JO, et al. Enhanced dissolution of ibuprofen using solid dispersion with poloxamer 407. *Arch Pharm Res.* 2008;31:1497–507.
38. Eloy JO, Marchetti JM. Solid dispersions containing ursolic acid in Poloxamer 407 and PEG 6000: a comparative study of fusion and solvent methods. *Powder Technol.* 2014;253:98–106.
39. Fouteris E, Tarantili PA, Karavas E, Bikiaris D. Poly(vinyl pyrrolidone)-poloxamer 188 solid dispersions prepared by hot melt extrusion: thermal properties and release behavior. *J Therm Anal Calorim.* 2013;113:1037–47.
40. Kumar S, Singh R, Gupta RN. Development of a single core osmotic tablet containing thermodynamically stable solid dispersion of nisoldipine. *Indian J Pharm Sci.* 2017;79:740–50.
41. Yu LX, Amidon GL, Polli JE, Zhao H, Mehta MU, Conner DP, et al. Biopharmaceutics classification system: the scientific basis for biowaiver extensions. *Pharm Res.* 2002;19:921–5.
42. Sachan N, Bhattacharya A, Pushkar S, Mishra A. Biopharmaceutical classification system: a strategic tool for oral drug delivery technology. *Asian J Pharm.* 2009;3:76.
43. Rajesh J, Rajendra D, Shrinivas M. Enhancement of solubility & dissolution rate of nifedipine by using novel solubilizer sepiatrap 80 & sepiatrap 4000. *J Drug Deliv Ther.* 2018;8:293–300.
44. Hecq J, Nollevaux G, Deleers M, Fanara D, Vranckx H, Peulen O, et al. Nifedipine nanocrystals: pharmacokinetic evaluation in the rat and permeability studies in Caco-2/HT29-5M21 (co)-cultures. *J Drug Deliv Sci Technol.* 2006;16:437–42.
45. Xie T, Taylor LS. Effect of temperature and moisture on the physical stability of binary and ternary amorphous solid dispersions of celecoxib. *J Pharm Sci.* 2017;106:100–10.
46. Lehmkemper K, Kyeremateng SO, Heinzerling O, Degenhardt M, Sadowski G. Impact of polymer type and relative humidity on the long-term physical stability of amorphous solid dispersions. *Mol Pharm.* 2017;14:4374–86.

Publisher's Note Springer Nature remains neutral with regard to jurisdictional claims in published maps and institutional affiliations.